LBL-13603
Preprint

Lawrence Berkeley Laboratory

UNIVERSITY OF CALIFORNIA

Materials & Molecular Research Division

RECEIVED
LAWRENCE
BERKELEY LABORATORY

APR 15 1983

LIBRARY AND
DOCUMENTS SECTION

Submitted to Surface Science

A COVALENT MODEL FOR THE BONDING OF ADSORBED HYDROCARBON FRAGMENTS ON THE (111) FACE OF PLATINUM

C. Minot, M.A. Van Hove, and G.A. Somorjai

December 1982

TWO-WEEK LOAN COPY

This is a Library Circulating Copy which may be borrowed for two weeks. For a personal retention copy, call Tech. Info. Division, Ext. 6782.

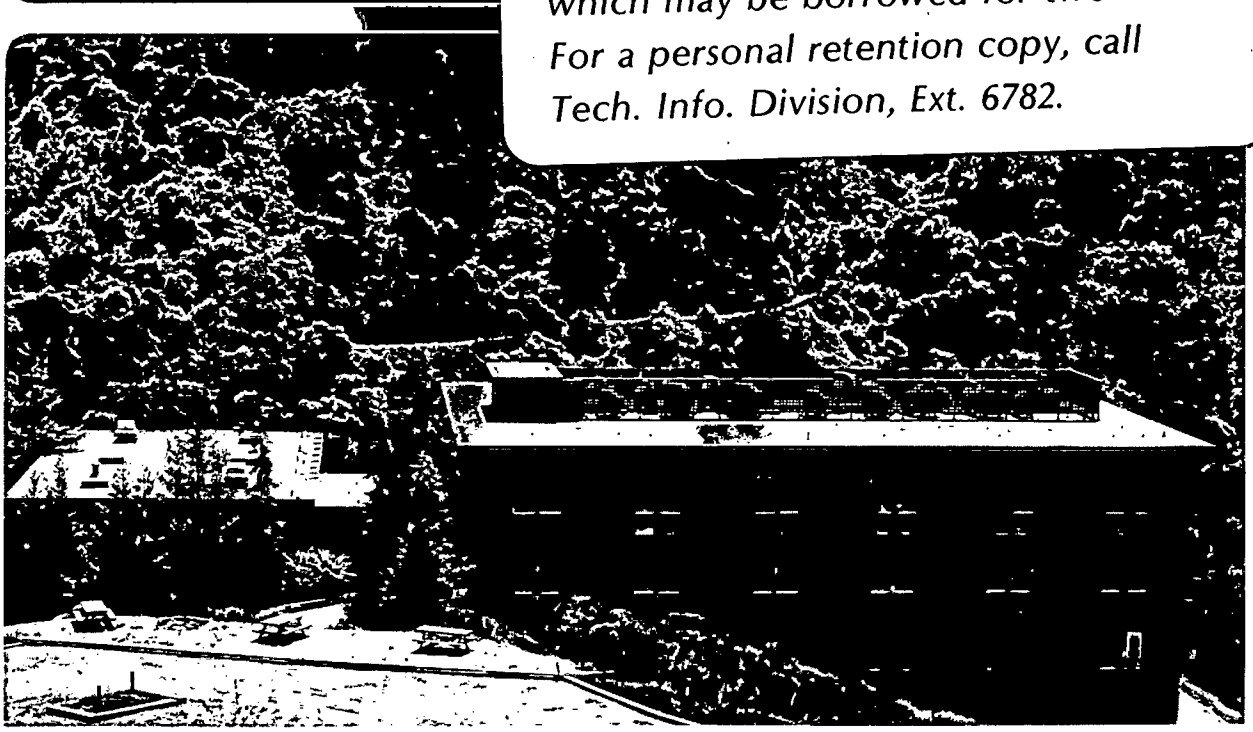

Prepared for the U.S. Department of Energy under Contract DE-AC03-76SF00098

LBL-13603

DISCLAIMER

This document was prepared as an account of work sponsored by the United States Government. While this document is believed to contain correct information, neither the United States Government nor any agency thereof, nor the Regents of the University of California, nor any of their employees, makes any warranty, express or implied, or assumes any legal responsibility for the accuracy, completeness, or usefulness of any information, apparatus, product, or process disclosed, or represents that its use would not infringe privately owned rights. Reference herein to any specific commercial product, process, or service by its trade name, trademark, manufacturer, or otherwise, does not necessarily constitute or imply its endorsement, recommendation, or favoring by the United States Government or any agency thereof, or the Regents of the University of California. The views and opinions of authors expressed herein do not necessarily state or reflect those of the United States Government or any agency thereof or the Regents of the University of California.

LBL 13603

A Covalent Model for the Bonding of Adsorbed Hydrocarbon Fragments on the (111) Face of Platinum

C. Minot,* M. A. Van Hove and G. A Somorjai

Materials and Molecular Research Division
Lawrence Berkeley Laboratory
and
Department of Chemistry
University of California
Berkeley, California 94720, USA

Abstract

A systematic molecular orbital study of the location of CH_n and $C-CH_n$ (n=1,2,3) species on a Pt(111) single-crystal surface has been performed by using an Extended Hückel Theory (EHT). These species may be involved in the hydrogenation/dehydrogenation processes of hydrocarbons. The observed dependence of the adsorption site on the number of hydrogens in the CH_n fragments suggests that any CH bond breaking in CH_n species must involve a change of adsorbate bonding site. The carbon is found to be located on the surface in such a way as to complete its tetravalency. Thus, CH occupies a 3-fold coordinated hollow site, CH_2 a 2-fold coordinated bridge site and CH_3 a 1-fold coordinated top site. $C-CH_3$ is found to be perpendicular to the surface in a 3-fold hollow site in agreement with experimental observations. It is also found that a displacement of $C-CH_2-R$ to a top site makes a β C-R cleavage easier.

---

*Permanent address: Laboratoire de Chimie Théorique, Bt. 490, Centre d'Orsay, Université de Paris-Sud, 91405 Orsay, France

INTRODUCTION

The structure of monolayers of unsaturated hydrocarbons on single crystal metal surfaces has been the subject of many investigations by a variety of experimental techniques over the last several years. For the most part, the metal substrates used were Pt(111)[1-31] and Ni(111)[12,15,16,22,32], and more recently Rh(111)[33-35] and Pd(111).[36] The hydrocarbons involved were mainly acetylene (C_2H_2), ethylene (C_2H_4), methylacetylene (C_3H_4), propylene (C_3H_6) and butene (C_4H_8). A variety of adsorption structures are formed at temperatures below about 400K, some of which have been found to consist of alkynes ($>C(CH_2)_nCH_3$). These alkynes were identified primarily with Low Energy Electron Diffraction (LEED), Ultraviolet Photoelectron Spectroscopy (UPS), High-Resolution Electron Energy Loss Spectroscopy (HREELS) and Thermal Desorption Spectroscopy (TDS). At higher temperatures sequential dehydrogenation of the hydrocarbon species occurs and CH_n fragments have been observed by HREELS and UPS on the surface (at still higher temperatures graphite structures can be formed). On Ni(111) surfaces the C-C bonds tend to break more easily than the C-H bonds, while the reverse is true on Rh(111) and Pt(111) surfaces.

These fragmented hydrocarbon surface structures are of great interest to aid the understanding of the elementary steps of bond breaking and catalysis. We seek to explore the connection between geometric structure (bonding arrangement, bond lenths and bond angles) and electronic structure (nature and occupation of electronic orbitals

involved in the metal-hydrocarbon bonding). A number of model calculations have been carried out already: most of them are concerned with the free organic molecules,[37] or with the adsorption site on flat and stepped surfaces,[38] or with the molecular conformation in the adsorbed state.[15,39-41] A calculation based on the Extended Hückel Theory (EHT) investigated the position of the CH_n fragments on a cluster of seven nickel atoms, representing the Ni(111) surface.[42] Other EHT calculations studied the bonding of acetylene and C_2H_n radicals on clusters representing Pt(111),[43-45] as well as Ni(111) and Rh(111)[44] crystal surfaces.

In this paper, we focus on the problem of finding the site of adsorption of each hydrocarbon fragment on a close-packed surface by using EHT.[46] For each possible site of adsorption, a cluster is chosen whose overall structural symmetry is the same as the short-range site symmetry; e.g., if a site with three-fold rotational symmetry is considered, the cluster will be given three-fold symmetry as well. Our aim in this study is to point out the major changes in the bonding interactions associated with a shift from one site on the surface to another and this will enable us to describe the metal-adsorbate bonds simply in terms of the coordination of the atoms of the adsorbate. Although the compact packing[47] of the metal substrate implies the availability of many d levels of each symmetry at each adsorption site, which at first sight suggests a flat energy surface, the adsorption site is found to affect the total energy substantially. This is because the interactions between the metal and the adsorbate depend on the local symmetry imposed by the position on the surface.[48] For

example, at a top site, a metal s orbital does not interact with an adsorbate orbital of symmetry e, whereas, at a threefold coordinated hollow site, the same s orbitals of the three metal atoms can combine to form a set of symmetry e appropriate for such an interaction.

To focus in such a way on the local metal-adsorbate interactions raises the question of the relevance of cluster calculations to the extended surface problem. For this reason, in Section 8, we report on tight-binding calculations that we have performed to check whether the introduction of the periodicity affects the results. These differ from EHT in their physical assumptions only in that the tight-binding calculations include the two-dimensional surface periodicity. It will emerge that our cluster calculations produce results that describe well the bonding of hydrocarbon fragments on extended surfaces.

2. Theoretical Methods

The cluster calculations have been carried out by using the ICON 8 program.[46,49] The off-diagonal hamiltonian matrix elements H_{ij} are derived from the diagonal terms using the weighted formula.[50] The method used for the band calculation is a crystalline extension of this program, within the tight binding scheme.[51] Its formalism is similar to the program used by Whangbo and Hoffmann.[52]

3. The Cluster Representation of the Surface

Two major questions arise in any cluster approach of modelling a surface. They stem from the way the cluster is bounded on the substrate side: How many atoms should the cluster contain? And how should the peripheral atoms be represented in the absence of many of their neighboring atoms?

The idea of a cluster to be used in adsorbate bonding calculations is justified by the observed strong structure sensitivity of the heat of adsorption.[53] Both surface thermodynamics and spectroscopic measurements on monolayer adsorbates indicate the predominance of localized bonding and nearest neighbor interactions.[53] Thus, only a few nearest neighbor metal atoms have an influence on the bonding of adsorbates. This allows us to limit the number of atoms inside the cluster.

We shall classify the substrate atoms according to their distance from the adsorbate site as illustrated in Fig. 1. Those metal atoms involved in chemical bonds with the adsorbate will be labelled M and represented as well as possible: we shall include all their valence orbitals (5d, 6s and 6p for Pt). In addition to their mutual M-M bonds, the atoms M are involved in M-M' bonds with atoms M' of the next shell of neighbors. The atoms M' affect the adsorbate-metal bonding through the hybridization of the M atoms. Inasmuch as we are only interested in the indirect effect of the atoms M' on the adsorbate-metal bonding, their description does not have to be as accurate as that of the atoms M. We therefore chose to represent the atoms M' only by their s orbitals. All atoms beyond the M' shell are ignored and we label them M". The s description for atoms M' is an advantage over the full description, not only because it limits the number of orbitals: it also partly resolves the boundary question. All the electrons of the atoms M' are involved either in the M-M' bonds or in the M'-M" bonds. If the unmatched electrons corresponding to the M'-M" bonds were included in the calculation, they would interfere with the M

system, implying charge transfers to the center of the cluster and thereby affecting the main interactions that we want to study. In this respect a set of monovalent atoms M' provides a good way of embedding the atoms M by preserving the topology of the environment without any M'M" bond. For that purpose, a set of plain s orbitals is the simplest approach. The next requirement is to choose this s orbital as similar as possible to the hybrid on the metal. This leads to choose the s orbital of the metal. It would have been possible to modify the parameters of the metal s orbital to decrease the polarization inside a 1M + 12M' cluster representing the bulk. There is however no need to do that because in this calculation the central atom appears to be nearly neutral: Pt(M) = 9.53 d + 0.47 s.

In fact, large clusters in which the M atoms are embedded in atoms M' represented by s orbitals have already been employed with pseudopotentials by Goddard and coworkers[54] and by Whitten and coworkers,[55] but the EHT method used here is sufficiently different from their approach that we cannot simply assume transferability of results.

Although our s-representation of the atoms M' simplifies the problem, it also introduces a new difficulty. If all the atoms are fully described, there is no problem in counting the electrons of the system, as both the number of electrons per atom and the number of atoms are then well defined. With the description of atoms M' by an s orbital only, the number of electrons per atom is a priori, however, undefined. The s orbitals in the bulk Pt are not empty and the number of electrons assigned to them should be a fractional number (in a band

structure sense) that depends on the nature of the M-M' bonds. Our solution to this problem is to choose the Fermi level as a cutoff between occupied and vacant orbitals, which we justify as follows.

The Energy Cutoff

If the metal cluster is chosen to be large enough, there is a large number of orbitals at the vicinity of the Fermi level E_f. The orbitals of the surface of the metal fragment whose energy is at the vicinity of E_f and whose symmetry allows mixing with the adsorbate levels, are shifted away from E_f. However, one can expect that in such a system many orbitals of improper symmetry for bonding remain near E_f. These allow us to define the highest occupied molecular orbital (HOMO) at the Fermi level, whatever the adsorbate. We therefore choose the energy cutoff in the middle of the band gap found for a cluster representing the bulk. Such a cluster we select as follows.

A tetrahedron of metal atoms is the largest finite cluster that consists of equivalent (and neutral) atoms. This cluster leads for platinum to an estimate of $-11.63 \pm .36$ eV for E_f, following the above procedure. As the number of energy levels in this cluster is limited, this value is, however, not very precise ($\pm$ .36 eV). A larger system of thirteen atoms composed of a central atom with its twelve nearest neighbors suffers some internal polarization but it exhibits a smaller gap between the relevant frontier orbitals, providing the same value for E_f with a smaller error, $-11.63 \pm .09$ eV. This value is used in our calculations. It corresponds in general to a large energy

gap in the system adsorbate + metal. This gap is a result of the formation of the bonds, which splits the bonding and the antibonding levels. However, the application of this second criterion for E_f (the largest gap) may change the electron counting by two (1 orbital) in some cases, namely the bridge-bonding systems. We shall later emphasize the effect of a modification of the energy cutoff with two specific examples.

In most of the cases discussed in this paper, $d_{x^2-y^2}$ and d_{xy} orbitals are close to the Fermi level. They have only a small spatial overlap with the adsorbate. These orbitals may be qualified as non-bonding with respect to the metal-adsorbate interaction. Therefore, to add or to subtract one electron in these orbitals does not change the metal-adsorbate interaction much. Such a possible change of the total number of electrons shows that our criterion for the determination of E_f is not too rigorous. A consequence is that, if we change the attribution of the charge of the adsorbate, all the major interactions with the metal will be preserved.

This model holds insofar as the energy cutoff lies in the gap between the bonding and the antibonding metal-adsorbate ligands. It can not apply to adsorbates whose electronegativity strongly differs from that of the metal, one hybrid not being involved in a two-electron interaction with the metal and therefore remaining either filled or empty. Then, the energy levels of the atoms would have to be changed to take into account the variation of electronegativity due to the charge polarization of such a system. This would reduce the difference between the energy of the hybrids and the Fermi level of the metal.

An iterative procedure leads to a model similar to Grimley's.[56] In our calculations this implies a change in the energy cutoff, which essentially corresponds to the necessity of taking the change of work function due to the adsorbate into account, when it is important. This is not the case for hydrocarbon adsorption: the E_{2p} level of the carbon (-11.4 eV) is not too far from our estimated Fermi level (-11.63 eV) so that the bonding and antibonding combinations of the hybrids are pushed away from this level. For simplicity we will count, in the case of a hydrocarbon fragment, that the sp hybrid pointing toward the surface is occupied and the p hybrid parallel to the surface is empty. This comes out from the atomic levels and is a formal way of counting, the only significant aspect being the population of bonding and antibonding orbitals of the whole system as resulting from the choice of the energy cutoff.

Geometries and Parameters

We shall now discuss the choice of cluster geometry and of parameters for our Extended Hückel calculations. The distinction between the atoms M and M' leads to a different cluster for each site of adsorption, since M represents metal atoms directly bonded to the adsorbate, cf. Fig. 1. Some CH_n and CCH_n species adsorbed at different sites are illustrated in Fig. 2. Bonding to a top site on the (111) face requires only one atom M and 9 atoms M'. Bonding to a bridge site leads to 2M and 13M'. The threefold site leads to 3M atoms and either 15 or 16 M' atoms, depending on the absence or presence of a second-layer metal atom directly below the hollow site (3-3 or 3-1

site, respectively). In this fashion, all the clusters are symmetry-adapted to the adsorption site.[49] A unique cluster for all adsorption sites would favor that site which has the same symmetry as the cluster itself, while for other sites, two locations equivalent by crystal symmetry would become different with respect to the symmetry of the cluster, and therefore would present artificially different interactions.

One can object to our choice that, by considering clusters of different sizes, the larger systems would always be energetically preferred because of the larger number of bonds present per atom. The orbital analysis suggests sometimes the contrary and the results of the calculations will show both cases: better adsorption on smaller or on larger clusters, depending on the case. We have fixed the carbon-platinum bond length at 1.9 Å for all adsorption geometries, as was done in reference 39, which is an average value based on relevant observed cluster geometries, as listed in Ref. 35. This constant bond length implies that the carbon atom is closer to the surface when above a threefold site than when above a top site, for example. We do not optimize this carbon-platinum bond length at each site because the differences would be very small and of little consequence.

The parameters we have chosen to represent the platinum atoms of type M are the same as in Ref. 57. The s orbital representing the atoms M' is exactly the same as the one used for the atoms M, as already mentioned.

4. The Nature of the Platinum-Platinum Interactions

The clean Pt(111) surface does not reconstruct, i.e., it has the structure expected from an ideal termination of the bulk lattice. A first test of our model is to see whether it can predict that a single Pt adatom will indeed be located on the (3-3) threefold site, extending the bulk ABC stacking of the layers. In fact, as the interaction energies in the top line of Table I show, the 3-3 hollow site does lead to the best result, the two hollow sites being better than the two other locations.

The question why a threefold rather than a top site consitutes the stronger binding site may be answered with simplicity by considering the interaction 1M-3M within a tetrahedron, with respect to the M-M interaction between two single atoms. In both cases, electron donation and back donation between atoms have to equilibrate, but in the tetrahedral case, each donation need not be individually compensated by an identical one. The relation between the fragments M and 3M may be seen as donor-acceptor interactions within a given symmetry, provided that the reverse relation exists in a different symmetry. The single atom is donor through its d_{xz} and d_{yz} orbitals. It will be easier to transfer these electrons to the e combination of s orbitals of the 3M system than to reach the p level of another 1M. In a parallel way, the single atom is acceptor through its s orbital and the a combination of dp_z orbitals pointing toward the hollow site makes the hollow site a better a donor than the single atom.

The choice of the 3-3 hollow site over the 3-1 hollow site may be understood from these relations by considering the perturbation of the

3M system due to the sublayer. The energy of the e combination of s orbitals of the 3M system is lowered by the interaction with the equivalent orbital of the sublayer in the 3-3 hollow case. This makes the 3M system a better e acceptor. Nothing like that appears with the sublayer in the 3-1 hollow case. The energy of the a combination of dp_z2 is lowered by the s orbital of the sublayer in the 3-1 case; this makes the 3M system a worse a donor with respect to the 3-3 case.

5. <u>The Nature of the Main Interactions Between Carbon and Platinum</u>

We shall restrict ourselves in this paper mainly to hydrocarbon orientations that are perpendicular to the surface. Considering the energy cutoff of -11.63 eV for a formal assignment of the electrons to the fragments, the hydrocarbons may be seen as possessing a filled a orbital (whose energy level varies from -13.30 eV for CH to -11.75 eV for CH_3) and in one case an empty π^* orbital (-11.4 eV for CH). This model holds for $\oplus CH$, CH_2, $\ominus CH_3$, $\oplus C-CH_3$, $C=CH_2$, $\ominus C=CH$ and CO. It can be extended to neutral fragments or to fragments with opposite charge as far as the frontier electrons are non-bonding (see the discussion on the energy cutoff in Section 3).

To build the complete system, the metal has to be considered with two opposing properties in mind, as follows. The metal should be an a <u>acceptor</u>, since the adsorbate is an a donor. Therefore, the <u>top site</u> is a better choice than the hollow site in which the small amplitude at the center of the in-phase combination does not lead to a good overlap with directional orbitals like p_z. Notice that this argument would not apply for hydrogen whose s orbital is not directional and overlaps better with M_3 than with an isolated atom M, by a ratio $\sqrt{3}$.

The metal should at the same time be an e donor to donate into an empty π^* orbital. This requirement, however, favors a hollow site. At the top site, the (d_{xz}, d_{yz}) orbitals are involved through a small π overlap. In a hollow site, two sets of orbitals d_{z^2} and (d_{xz}, d_{yz}) are involved through a larger atomic σ overlap. In cases where the e interactions are important, the carbon will prefer to be involved in three single bonds in a hollow site rather than in a triple bond on a top site. This occurs with CH. If one of the two e orbitals is missing, as in CH_2, the bridge site allows the interaction with the remaining p_c orbital on the carbon atom to be preserved. This argument also determines the bonding geometry. The p_c orbital has to be parallel to the metal-metal bond to interact with the out of phase combination of the d_{z^2} and d_{xz} orbitals. So the staggered tetrahedral conformation of M_2CH_2 is better than the eclipsed planar one. Our calculations lead to a difference of 1.2 eV between these two. In CH_3 the two p orbitals are missing and the a interactions favor the top position.

The result is that the carbon binds at a site such that it saturates its coordination: CH on a threefold site, CH_2 on a bridge site and CH_3 on a top site all lead to tetravalent carbons, as illustrated in Fig. 2. Moreover the conformation of CH_2 on the bridge site leads to the choice of a tetrahedrally coordinated carbon over a planar coordinated carbon.

As is shown in Table II, our calculations predict that the adsorption on the (100) face is very similar to that on the (111) face.

The adsorption energies are only slightly weaker on (100). The top sites behave the same way on both faces and the fourfold site can provide an e set of orbitals similar to the e set of the three fold site. This leads to a pentavalent instead of a tetravalent carbon on (100) and shows a limitation of the simple rule of the saturation of the adsorbate coordination.

6. Results of EHT Cluster Calculations for Adsorbed CH_n Fragments

Table I, in which metal-hydrocarbon interaction energies are reported, confirms the trend outlined in the previous section. We shall now examine these results in more detail.

In Table IV are reported the sum of the overlap populations for the M-C bonds for each symmetry a and e in the $\oplus$CH system. These values confirm that the a bonding is larger for the top position and that the e bonding is larger for the hollow position. Similarly, the largest depopulation of the a orbitals of the metal is observed on top sites and the increase in population of the e orbitals of the hydrocarbon is largest on hollow sites.

In Table I are also reported the results concerning $\oplus CH_3$. Its location on the surface is similar to that of $\ominus CH_3$. However, the adsorption energies are different, indicating that the frontier orbital is non-bonding. Within the a symmetry, three orbitals interact: the sp_3 hybrid of the carbon, the s and the d_{z^2} orbitals of the metal. This leads to a low bonding orbital which mainly accounts for the σ donation to the metal. Its variations impose the choice of the site of adsorption. The second one is roughly non-bonding and lies at the Fermi level. It is occupied for $\ominus CH_3$, and becomes empty for $\oplus CH_3$.

In a more detailed analysis, this orbital is slightly antibonding, due to the repulsion between sp_3 and d_{z^2}. If we remove two electrons from the system, the energy of adsorption, which should not be affected by the frontier orbital if it were purely non-bonding, is uniformly increased by about 1 eV. However, this has a minor influence on the choice of the site of adsorption. This illustrates that the position is mostly due to deep orbitals not affected by a change in the electron counting.

Overlap Population of CH Bonds in CH + Metal

According to Table IV, the overlap population of the CH bond does not vary from one site to another. All the values remain close to the value of the fragment alone (.785). The most deviating value (.769) corresponds to the largest interaction in the a system, i.e., to the top site. The electronic transfer from the two a occupied orbitals of CH (σ_{pair} and σ_{CH}) decreases the overlap population because of their bonding CH character. The decreases are .092 and .039, respectively. The donation to the σ^*_{CH} leads to a further decrease of .013. Therefore the polarization[57] of the system is responsible for restoring the bond strength almost completely. It induces an increase in the overlap population by .128 with the dominant contribution of .141 due to the large mixing of the σ_{pair} with σ_{CH}. (The partial overlap of these two orbitals involved in the C-H bond is very large: .789.)

The mixing of the two fragment orbitals σ^o_{CH} and σ^o_{pair} in each perturbed MO is governed by the interactions with the metal. These interactions impose for σ_{CH} the phase of s_C and for σ_{pair}

the phase of p_C. Referring now to the character of the bond between C and H, the lowest MO ($\sigma_{CH} + \sigma_{pair}$) is antibonding and the highest MO ($\sigma_{pair} - \sigma_{CH}$) is bonding. The ratio of the two mixings is in inverse proportion to the energy gap between the initial energy level and the metal energy level. The largest mixing occurs in the highest orbital, which is the bonding one; therefore the bonding character dominates and the polarization increases the C-H overlap population.

In a perhaps more pictorial way (Fig. 3) one can summarize the polarization as 1) delocalizing σ^o_{CH} to build a pseudo-symmetrical MO σ_{MCH} whose bonding character is shared between MC and CH instead of being relevant to CH alone; 2) delocalizing the σ^o_{pair} more, to construct a pseudo-antisymmetric MO. This eliminates the s coefficient on the carbon and the $s_C - s_H$ antibonding character. This loss of antibonding character prevails.

Overlap Population of CH Bonds in CH_3 + Metal

The σ system of CH_3 behaves as in the $^{\oplus}CH$ case and therefore we do not expect a large variation of the overlap population (see previous section). In the top site, the electronic transfers are responsible for a decrease of the overlap population matrix of .017, which is over-compensated by an increase of .024 due to the polarization. This leads to a net increase of .007 which is small.

What is new in $^{\ominus}CH_3$ with respect to $^{\oplus}CH$ is that the CH bonds are involved in the π system. The backdonation from the e orbitals of the metal fills the π_{CH} orbitals which are antibonding. So if this backdonation is important, the carbon-hydrogen bonds become weaker.

Since the backdonation is not as important in the top site as it is in the hollow site, one can expect that the overlap population is much more decreased in the latter case. These results of our calculations are reported in Table V.

The π contributions of the overlap population show a decrease of .008 on top and a decrease of .084 on hollow. This suggests that if the methyl is located on the three fold site, it will undergo more easily a decomposition to CH. The construction of the bonds between the metal and the carbon is made at the expense of the CH bonds.

For CH_3, the 3-3 hollow site leads to a value of the overlap population of CH (.717) which is very close to that for the 3-1 hollow site (.715). The bridge site leads to two different values: one of them (.769) is close to the top value (.785) and the other (.716) is quite similar to the hollow values.

7. Results of EHT Cluster Calculations for Adsorbed C_2H_n Fragments, $\geqslant C-CH_3$ and Other Alkylidynes

As shown in Table I, the absorption of $\oplus CCH_3$ is very similar to the adsorption of $\oplus CH$. The best location is in the hollow site. For this site the rotational barrier of the methyl group is .032 eV within our model, which is small compared to that of ethane (0.13 eV). However, contrary to the $\oplus CH$ case, the backdonation affects the C-C bond. Overlap populations of CC and CH bonds are reported in Table VI. The empty p_C orbitals mix with the occupied π_{CH} within the fragment $\oplus CCH_3$, stabilizing the CC bond and destabilizing the CH bonds. The back donation from the metal raises the p_C level and decreases this

interaction. It follows that the $p_C-\pi_{CH}$ interaction is mostly apparent when CCH_3 is on top where the back donation is weak. Then, the system can dissociate more easily by losing its hydrogens. On the other hand, when CCH_3 occupies the threefold site (the best one, also found experimentally), the system M_3CCH_3 resembles ethane more, with a weakened CC bond and strengthened CH bonds. Such a system would not lead to an easy dehydrogenation.

A shift from the most stable position (hollow) to the least stable one (top) leads to a β cleavage. (We use the conventional labelling α,β,γ,... to designate bonds of increasing distance from a given atom; in our case, with for example the $M-C_1-C_2-C_3$ skeleton, the α-,β- and γ-bonds are, respectively, the C_1-C_2, C_2-C_3 and C_3-C_4 bonds.) Such a β cleavage gives the α CC bond a multiple bond character which favors the location on top. If present, a δ bond could also participate, stabilizing the fragment and making the cleavage easier. The shift on the surface to a top site reduces the back donation, weakening the δ bond together with the β bond and strengthening both the α and the γ bonds.

The C-C bond breaking has been observed in thermal desorption experiments,[21] in which the hydrogen desorption rate from the surface (which should be about proportional to the C-H bond breaking probability) is monitored as a function of increasing surface temperature. These experiments were carried out with butenes, propylenes and acetylenes adsorbed on Pt(111), which are believed to form alkylidyne surface species[20] ($\rightarrow C-CH_2-CH_2-CH_3$, $\rightarrow C-CH_2-CH_3$ and

$\rightarrow C-CH_3$, respectively). The results reveal that the C-C breaking in the different adsorbed molecules occurs with increasing ease (i.e., decreasing temperature) in the order butene < propylene < ethylene ≅ acetylene. These experiments are consistent with a dehydrogenation occurring in top sites. The α cleavage is the only possiblity for a C_2 specie and it is the least likely one. We assume the observed CC breaking from propylene and butene to be a β cleavage. The presence of δ bonds then makes the breaking easier for the butene.

<u>$-C\equiv CH$ and $>C=CH_2$</u>

The $-C\equiv CH$ species has not been identified experimentally on Pt(111), but is a likely intermediate in several processes, such as transformation of adsorbed acetylene to adsorbed ethylidyne or dehydrogenation of this ethylidyne. The results of our calculations (Table I) show a slight difference between the various sites of adsorption for the $-C\equiv CH$ species. The bridge site and the top site are more favorable than the two hollow sites. (The CC distance has been taken to be 1.2 Å for all sites.) The difference between the various sites must remain smaller than for $\ominus CH_3$: the carbon, being involved in π bonding instead of σ bonding, is more sensitive to the backdonation.

All the above results concern the geometry perpendicular to the surface. The saturated compound $C-CH_3$ has no reason to deviate from this geometry. However, $-C\equiv CH$ and $>C=CH_2$, presenting an unsaturation at the β carbon, may be expected to bend toward the surface to yield another metal-carbon interaction.

According to our calculations, every deviation from the perpendicular geometry destabilizes the system, as shown in Table VII. This destabilization remains even if we bend the C_α-C_β axis to the extent that the C_β bonds to the metal with a distance of 1.9 Å (the destabilizations are .107 eV for the 3-1 hollow/top combination and .133 eV for the 3-3 hollow/top combination).

Such bent geometries could, however, be expected on the basis of those postulated for acetylene on Ni(111).[29] The predominance of the perpendicular geometry here contrasts with the situation occurring in cobalt clusters[59] analyzed by Schilling and Hoffmann.[60] For the closest possible comparison with Schilling and Hoffmann's results, we calculate the geometry of CCH_2 in a threefold site (3-1 hollow) and again the perpendicular geometry is more stable than the best bent geometry (by .388 eV).

The difference with the cobalt cluster is that the two-electron attractive interaction that they observed turns out to be a four-electron repulsive interaction on the Pt surface. The p orbital of the β-carbon is found to be slightly bonding and below the Fermi level. Therefore it is occupied and is repelled by the surface. On the cobalt cluster, the equivalent orbital is vacant and an attraction by the metal results. In order to prove that, we have lowered our energy cutoff by removing four electrons from the system. Then the interaction becomes a 2-electron attractive interaction and the bent geometry becomes more favorable by .264 eV.

Ni, Pd and Pt are too rich in electrons to produce these interactions. Removing 4 electrons from a 3M cluster corresponds to a

shift in the periodic table by one column. This leads to Co, Rh, and Ir in which the bent conformation would be more likely, as observed on the cobalt clusters.

8. Tight Binding Calculations

In order to investigate whether the introduction of the two-dimensional surface periodicity could change the results derived from an EHT cluster calculation, we have performed tight binding calculations of ⊕CH, CH_2 and ⊖CH_3 adsorbed on a 6-atom thick layer of platinum. The evaluation of the overlap and Hamiltonian matrices remains similar to that for the cluster calculations. The parameters are also the same except for the level of the 5s orbital of the platinum which has been set to -10 eV instead of -9.077 eV to produce a better result for the calculation of bulk platinum.

The adsorbate superlattice is assumed to be $(\sqrt{3} \times \sqrt{3})$ R30°, corresponding to a 1/3 monolayer coverage. The unit cell includes 18 atoms of platinum distributed in 6 planes and one adsorbate fragment (on one side of the metal layer only). Nine points in k-space representing a grid in the irreducible Brillouin zone have been chosen as shown in Table VIIIa. The Fermi level is found at 10.978 eV for the adsorbate-free surface. It does not vary much for the surface plus adsorbate systems (Table IX).

In Table VIII are reported the differences of adsorption energy at each k point for the same adsorbate at two different locations on the surface. They confirm the site preferences that we found with the cluster calculations.

It may happen sometimes that a level crosses the Fermi level for some position on the surface and does not for another, introducing a difference of two in the electron count at a given k point. This occurrence is compensated by an opposite difference at another k point. Insofar as we only consider the energies, we choose to balance the number of electrons between each geometry when necessary by adding or by removing two electrons at the Fermi level. This means that we focus our attention on total energies only and so do not introduce a significant error, because there is a higher density of states near the Fermi level. More so than in cluster calculations, there is always at a surface a great number of orbitals near the Fermi level (the unit cell introduces a total of 162 orbitals in one of our cases). These orbitals are pure metal orbitals and do not give significant bonding or antibonding interactions between the metal and the adsorbate.

From Tables VIIIb and VIIIc one can conclude that whatever the k point is, $\ominus CH_3$ is better on a top site and $\oplus CH$ on a threefold site. This result confirms what has been found by cluster calculations. The top-site preference for the methyl group is the largest at the point $\Gamma(0,0)$. The wavefunction at this point is the most symmetrical with no nodes and is the best for providing an a interaction. The threefold site preference of the CH group is largest at the point (1/3, 1/3) which introduces nodes in two dimensions and seems therefore convenient for an e interaction. If that is true, the same reasoning implies that the point (0,1/2) would be the best for the bridge site. Tables VIIIf and VIIIg show indeed that when the bridge site is the most

favorable one (with CH_2), this k point has the largest predominance. In tables VIIId and VIIIe, it is shown that the bridge position is intermediate between the best and the worst position for CH and CH_3, again confirming a trend noted for the cluster calculations.

9. Conclusions

The results of the tight binding calculations confirm those of the cluster calculations as models for hydrocarbon chemisorption on metal surfaces. Both kinds of calculation justify the assumption that the driving force for the determination of the coordination site is the formation of chemical bonds between the adsorbate and a very limited number of metal atoms.

The fragments of organic molecules adsorb strongly to the metal to replace their lost bonding partners by substitution with the metal. Their unsaturated atoms position themselves on the surface in such a manner as to be linked through single bonds to the closest metal atoms and thereby recover their saturation. This preference determines both the adsorption site and the molecular orientation. The adsorbed fragment, as opposed to a gas-phase fragment, thus resembles the saturated molecule. It is therefore relatively stable. This also implies that it is less distorted than the gas-phase fragment, the general statement being that the adjacent (α) bonds to the surface are strengthened and the next-farther (β) bonds weakened. From this model of adsorption, it follows that the hydrogenation-dehydrogenation

processes involve shifts from site to site along the surface, since any bond broken or formed in the adsorbate implies another coordination and therefore another site.

The predictions of our calculations are in general agreement with the limited set of experimental data available on these adsorbed hydrocarbon fragments and should help understand the elementary chemical bonding and reaction processes that occur at metal surfaces.

Acknowledgements

We are grateful for very useful discussions with and suggestions by Prof. L. Falicov, Mr. J. Tersoff and Mr. R. J. Koestner at Berkeley and have benefitted from further discussions with Mr. T. Hughbanks at Cornell University. This work was supported by the Director, Office of Energy Research, Office of Basic Energy Sciences, Materials Science Division of the U.S. Department of Energy under Contract No. DE-AC03-76SF00098. One of us (C.M.) acknowledges partial financial support by NATO.

References

1. L. L. Kesmodel, P. C. Stair, R. C. Baetzold and G. A. Somorjai, Phys. Rev. Lett. 36, 1316 (1976).
2. P. C. Stair and G. A. Somorjai, Chem. Phys. Lett. 41, 391 (1976).
3. H. Ibach, H. Hopster and B. Sexton, Appl. Surf. Sci. 1, 1 (1977).
4. H. Froitzheim, H. Hopster, H. Ibach, and S. Lehwald, Appl. Phys. 13, 147 (1977).
5. H. Ibach, H. Hopster and B. Sexton, Appl. Phys. 14, 21 (1977).
6. J. E. Demuth, Chem. Phys. Lett. 45, 12 (1977).
7. L. L. Kesmodel, P.C. Stair, and G. A. Somorjai, Surf. Sci. Lett. 64, 342 (1977).
8. L. L. Kesmodel, P. C. Stair, R. C. Baetzold and G. A. Somorjai, Surf. Sci. 66, 299 (1977).
9. W. J. Lo, Y. W. Chung, L. L. Kesmodel, P. C. Stair, and G. A. Somorjai, Sol. St. Commun. 22, 335 (1977).
10. P. C. Stair, and G. A. Somorjai, J. Chem. Phys. 66, 2036 (1977).
11. H. Ibach and S. Lehwald, J. Vac. Sci. Technol. 15, 407 (1978).
12. J. E. Demuth, H. Ibach and S. Lehwald, Phys. Rev. Lett. 40, 1044 (1978).
13. L. L. Kesmodel, L. H. Dubois, and G. A. Somorjai, Chem. Phys. Lett. 56, 267 (1978).
14. L. L. Kesmodel, L. H. Dubois, and G. A. Somorjai, J. Chem. Phys. 70, 2180 (1979).
15. J. E. Demuth, Surf. Sci. 80, 367 (1979).
16. J. E. Demuth, Surf. Sci. 84, 315 (1979).

17. F. P. Netzer and J.A.D. Matthew, Sol. St. Commun. 29, 209 (1979).

18. L. H. Dubois, D. G. Castner and G. A. Somorjai, J. Chem. Phys. 72, 5234 (1980).

19. T. E. Felter and W. H. Weinberg, Surf. Sci. 103, 265 (1981).

20. R. J. Koestner, J. C. Frost, P. C. Stair, M. A. Van Hove and G. A. Somorjai, Surf. Sci. 116, 85 (1982).

21. M. Salmeron and G. A. Somorjai, J. Phys. Chem. 86, 341 (1982).

22. J. E. Demuth and D. E. Eastman, Phys. Rev. Lett. 20, 1123 (1974).

23. J. E. Demuth and D. E. Eastman, Phys. Rev. B13, 1523 (1976).

24. J. E. Demuth, Surf. Sci. 69, 365 (1977).

25. J. E. Demuth, Surf. Sci. 76, L603 (1978).

26. J. E. Demuth and H. Ibach, Surf. Sci. 78, L238 (1978).

27. M. G. Cattania, M. Simonetta and M. Tescari, Surf. Sci. 82, L615 (1979).

28. J. C. Bertolini and J. Rousseau, Surf. Sci. 83, 531 (1979).

29. J. E. Demuth and H. Ibach, Surf. Sci. 85, 365 (1979).

30. S. Lehwald and H. Ibach, Surf. Sci. 89, 425 (1979).

31. P. Klimesch and M. Henzler, Surf. Sci. 90, 57 (1979).

32. S. Lehwald, W. Erley, H. Ibach and H. Wagner, Chem. Phys. Lett. 62, 360 (1979).

33. D. G. Castner, B. A. Sexton and G. A. Somorjai, Surf. Sci. 71, 519 (1978).

34. L. H. Dubois, D. G. Castner and G. A. Somorjai, J. Chem. Phys. 72, 5234 (1980).

35. R. J. Koestner, M. A. Van Hove and G. A. Somorjai, to be published.

36. J. A. Gates and L. L. Kesmodel, J. Chem. Phys. 76, 4281 (1982).

37. W. H. Weinberg, H. A. Deans, and R. P. Merrill, Surf. Sci. 61, 312 (1974).

38. H. Kobayashi, S. Yoshida, H. Kato, K. Fukui, K. Tarama and M. Yamaguchi, Surf. Sci. 97, 329 (1980).

39. R. C. Baetzold, Chemical Physics 38, 313 (1979).

40. J. E. Demuth, IBM J. Res. Develop. 22, 265 (1978).

41. R. E. Felter and W. H. Weinberg, Surf. Sci. 103, 265 (1981).

42. R. M. Gavin, J. Reutt, and E. L. Muetterties, Proc. Natl. Acad. Sci. USA, 78, xxxx (1981).

43. A. Gavezzotti and M. Simonetta, Surf. Sci. 99, 453 (1980).

44. A. Gavezzotti, E. Ortoleva and M. Simonetta, J. Chem. Soc. Faraday Trans. 1, xx, xxx (1981).

45. A. B. Anderson and A. T. Hubbard, Surf. Sci. 99, 384 (1980).

46. R. Hoffmann, J. Chem. Phys. 39, 1397 (1963).

47. A. B. Anderson and R. Hoffmann, J. Chem. Phys. 61, 4545 (1974).

48. C. Minot, O. Kahn, and L. Salem, Surf. Sci. 94, 515 (1980).

49. R. Hoffmann, W. N. Lipscomb, J. Chem. Phys. 36, 2179, 3489 (1962); 37, 2872 (1962).

50. R. Hoffmann, P. Hofmann, J. Amer. Chem. Soc., 98, 598 (1976); J. H. Ammeter, H. Bürgi, J. Thibeault, R. Hoffmann, ibid 100, 3686 (1978).

51. J. M. André, J. Chem. Phys. 50, 1536 (1969).

52. M. H. Whangbo, R. Hoffmann, J. Amer. Chem. Soc., 100, 6093 (1978); M. H. Whangbo, H. J. Foshee, R. Hoffmann, Inorg. Chem. 19, 1723 (1980).

53. G. A. Somorjai, "Chemistry in Two Dimensions: Surfaces," Cornell University Press, Ithaca, N.Y. (1981).

54. V. Avdeev, T. Upton, W. H. Weinberg, and W. A. Goddard, Surf. Sci. 95, 391 (1981); T. Upton and W. A. Goddard, Phys. Rev. Lett. 62, 472 (1979); C. F. Melius, T. Upton and W. A. Goddard, J. Vac. Sci. Technol. 18, 531 (1979); C. F. Melius, T. Upton and W. A. Goddard, Sol. St. Commun. 28, 501 (1978).

55. T. Pakkanen and J. L. Whitten, Phys. Rev. B21, 4357 (1980).

56. T. B. Grimley, Proc. Phys. Soc. 90, 751 (1967); 92, 776 (1967).

57. R. H. Summerville and R. Hoffmann, J. Am. Chem. Soc. 98, 7240 (1976); A. Dedieu and R. Hoffmann, J. Am. Chem. Soc. 100, 2074 (1978).

58. L. Libit and R. Hoffmann, J. Am. Chem. Soc. 96, 1370 (1974); S. Inagaki, H. Fujimoto and K. Fukui, J. Am. Chem. Soc. 98, 4054 (1976).

59. D. Seyferth, G. Williams, and J. Hallgren, J. Am. Chem. Soc. 95, 266 (1973); D. Seyferth, G. Williams and D. D. Traficante, J. Am. Chem. Soc. 96, 604 (1974); D. Seyferth, Adv. Organomet. Chem. 14, 97 (1976).

60. B. Schilling, and R. Hoffmann, J. Am. Chem. Soc. 100, 6274 (1978); 101, 3456 (1979).

Figure Captions

Figure 1. Metal clusters used to model the substrate around three different adsorption sites. Atoms M are nearest neighbors of and directly bonded to the adsorbate. Atoms M' are the non-M nearest neighbors of the atoms M. Lines connect atoms in the topmost surface layer, while the other atoms are in the second metal layer.

Figure 2. Preferred adsorption sites of CH, CH_2, CH_3, CCH_3, CCH_2 and CCH on Pt(111). Sphere radii have no physical significance.

Figure 3. Interactions of type a in CH + M.

Table I. Metal-adsorbate interaction energies on Pt(111)(in eV)
E(cluster + adsorbate) - E(cluster) - E(adsorbate)

The C-C distances are 1.52, 1.34, and 1.20 Å for $^{\oplus}CCH_3$, $^{\ominus}CCH_2$ and $^{\ominus}CCH$, respectively, while the nearest-neighbor Pt-C distances are all 1.90 Å.

Adsorbate	Top	Bridge	3-1 hollow	3-3 hollow
Pt	.329	.537	.617	.633
$^{\oplus}CH$	3.89	5.85	6.73	6.71
CH_2	.108	3.90	2.77	2.76
$^{\ominus}CH_3$	1.74	.555	-1.20	-1.00
$^{\oplus}CH_3$	2.58	1.59	.388	.400
$^{\oplus}CCH_3$	3.55	5.26	5.96	5.94
$^{\ominus}CCH_2$	7.90	9.30	---	8.94
$^{\ominus}CCH$	3.25	3.20	2.58	2.62

Table II. Adsorption energies (eV) of CH and CH_3 fragments chemisorbed on Pt(100) and Pt(111).

	CH	CH_3
Top (100)	3.75	1.64
Top (111)	3.89	1.74
4-fold (100)	5.96	-1.20
3-fold (111)	6.73	-2.13

Table III. Electronic transfer inside the tetrahedron (4M = 3M + M)

Symmetry:	A	E	A_2
Electronic Transfer:			
3M ---> M	.138	.046	---
M ---> 3M	.061	.104	.018

Table IV. Overlap populations ΣL_{MC} and ΣL_{CH} of ⊕CH on platinum and densities of electrons $\Sigma\psi^2$. $\Sigma\psi_1^2$ is the population of the a orbital of the metal, which is smallest on the top site; $\Sigma\psi_2^2$ is the population of the e orbital of ⊕CH, which is largest on the hollow sites.

	Symmetry	Top	Bridge	3-1 hollow	3-3 hollow
ΣL_{MC}	A	.402	.309	.384	.350
ΣL_{MC}	E	.149	.233	.311	.335
$\Sigma\psi_1^2$	A	.66	--	.98	.91
$\Sigma\psi_2^2$	E	.49	.84(.60)	.80	.80
ΣL_{CH}		.769	.775	.779	.777

Table V. Overlap populations of $\ominus CH_3$

	CH_3 Isolated	CH_3 On Top	CH_3 On 3-1 hollow
σ	.279	.286	.292
π	.507	.499	.423
$(\sigma + \pi)$	.786	.785	.715

Table VI. Overlap population L_{CC} and L_{CH} for the system $C-CH_3$ and decomposition in σ and p contributions

	CCH_3	Top	Bridge	3-1 hollow	3-3 hollow	C_2H_6
L_{CC}	.899	.832	.832	.779	.776	.732
π	.067	.046	.036*(.020)	.018	.018	-.009
σ	.765	.741	.766	.743	.740	.753
L_{CH}	.744	.761	.766*(.774)	.779	.779	.792
π	.469	.481	.487	.497	.498	.511
σ	.275	.280	.279	.282	.282	.281

* The first value refers to the hydrogen whose orientation is perpendicular to MM.

Table VII. Differences in energy (eV) between the perpendicular absorbate -C≡CH and the bent absorbate with an angle of 60° between the molecular axis and the surface normal.

C_α indicates the adsorption site, while C_β defines the azimuthal orientation of the bending by indicating the site nearest to the β carbon. The CCH geometry has been kept linear.

	C_α	top	top	bridge	bridge
Perpendicular	C_β	top	bridge	top	hollow
	ΔE	-.595	-.572	-.224	-.389
	C_α	3-1 hollow	3-1 hollow	3-3 hollow	3-3 hollow
Bent	C_β	top	bridge	top	bridge
	ΔE	-.261	-.360	-.135	-.386

Table VIIIa. Weights (upper lines) and coordinates in k-space (lower lines) of the nine calculated points in the irreducible section of the Brillouin zone for a $(\sqrt{3} \times \sqrt{3})R30^\circ$ structure. The coordinates are given in terms of two substrate lattice vectors (parallel to the surface) oriented 120° to each other.

				1/16 (1/2,1/2)
		1/8 (1/4,1/4)	1/4 (1/3,5/12)	1/8 (5/12,7/12)
1/48 (0,0)	1/8 (1/12,1/6)	1/8 (1/6,1/3)	1/8 (1/4,1/2)	1/24 (1/3,2/3)

VIIIb) Energy difference (eV) between CH in threefold and in top sites for the various k-points of Table VIIIa. The threefold site is preferred. The average difference is 2.53 eV.

				2.81
		2.06	2.59	3.19
1.70	1.77	2.23	2.91	3.63

VIIIc) As in b) for CH_3. The top site is preferred. The average anergy difference is -3.22 eV.

				-2.81
		-3.74	-3.43	-2.12
-3.89	-4.12	-3.51	-2.78	-1.72

VIIId) CH:difference threefold-bridge site.* The threefold site is preferred. The average difference is .83 eV.

				.91
		.53	.89	1.11
.23	.22	.89	1.04	1.80

VIIIe) CH_3:difference top-bridge site.* The top site is preferred. The average difference is 1.73 eV.

				1.09
		2.25	1.69	.77
2.68	2.73	1.95	1.53	.68

VIIIf) CH_2:difference bridge-top site. The bridge site* is preferred. The average difference is .47 eV.

				2.49
		.00	.33	.94
.03	-.08	.12	.50	1.01

VIIIg) CH_2:difference bridge-hollow site. The bridge site* is preferred. The average difference is .85 eV.

				3.18
		.57	.72	.49
1.63	1.11	.61	.63	.24

* The bridge conformation is perpendicular to M_2 leading to a tetrahedral carbon, which is better by 2.15 eV than the parallel conformation leading to a square planar carbon.

Table IX. Variation of Fermi level (eV) with adsorbate and adsorption site in tight binding calculations.

	Pt alone	10.978
$\oplus CH$	top	10.913
	bridge	10.941
	hollow	10.936
$\ominus CH_3$	top	10.891
	bridge	10.869
	hollow	10.861

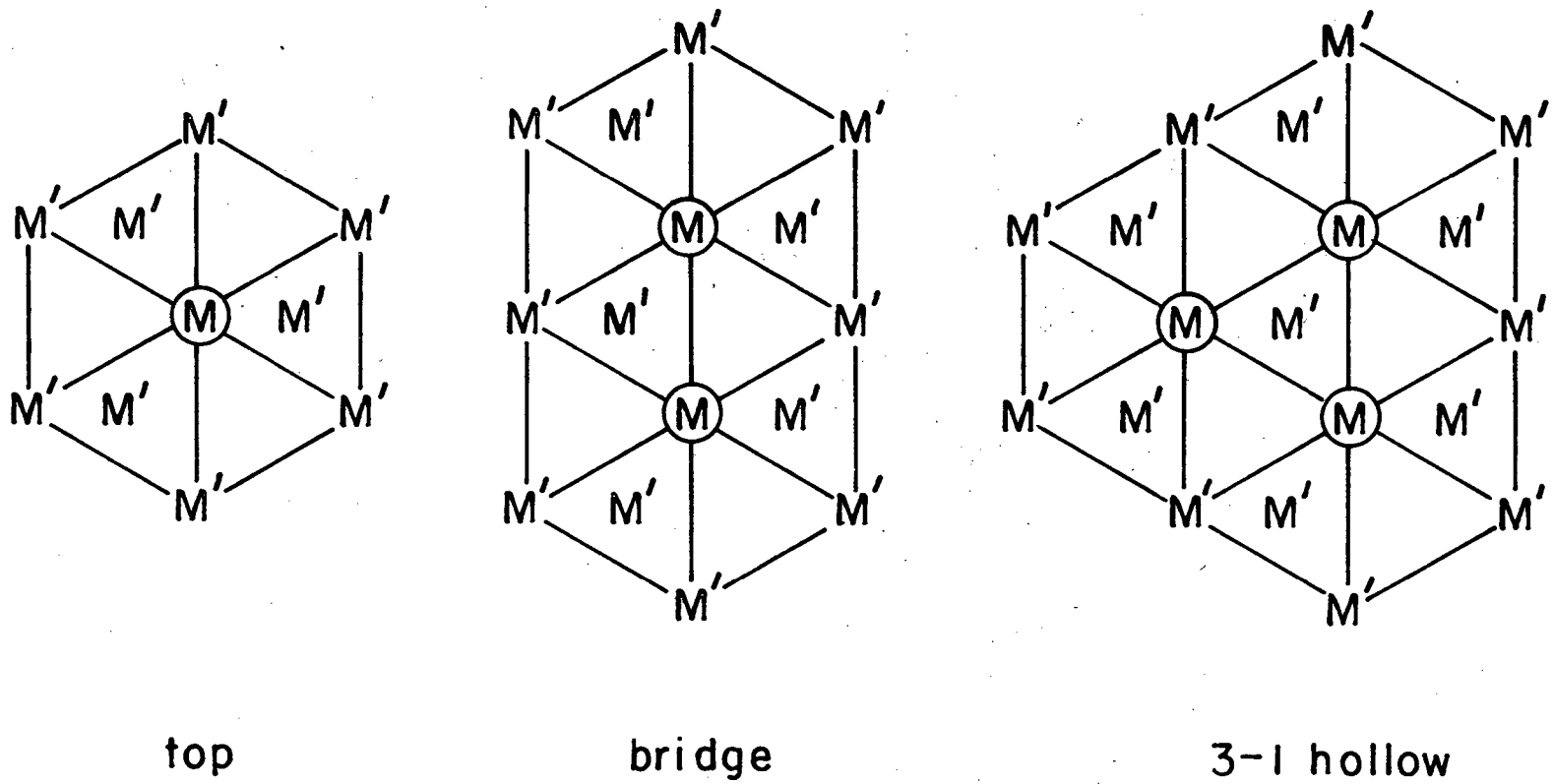

Fig. 1

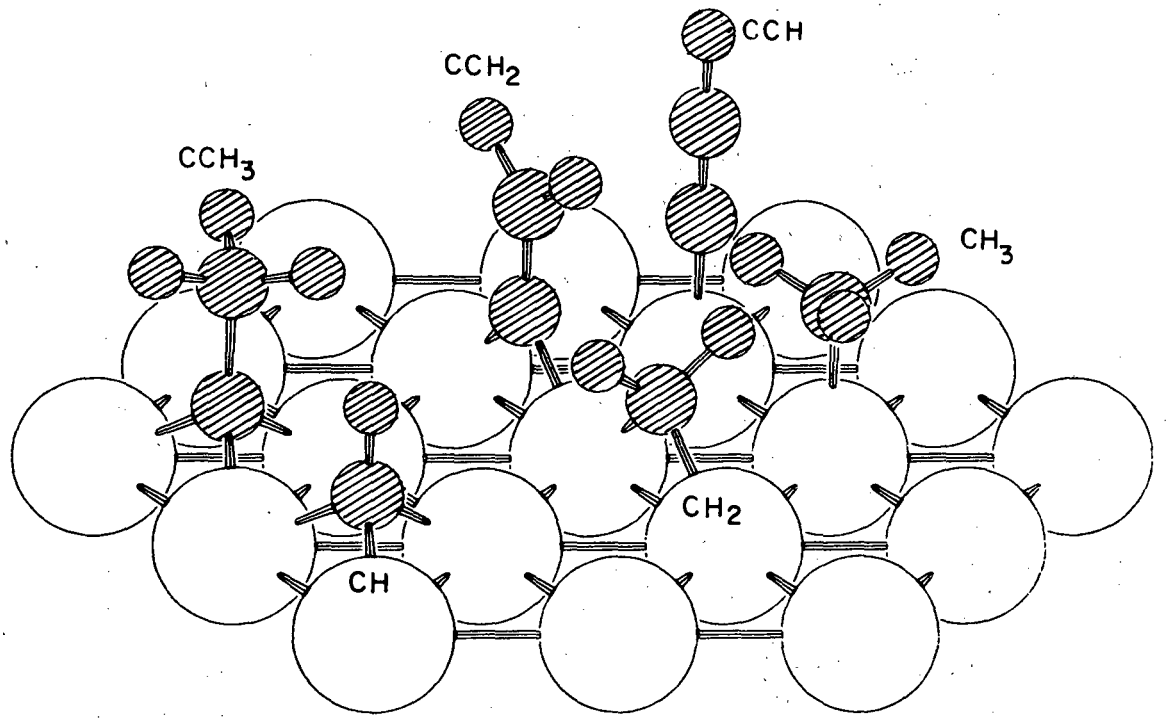

XBL 826-5941

Fig. 2

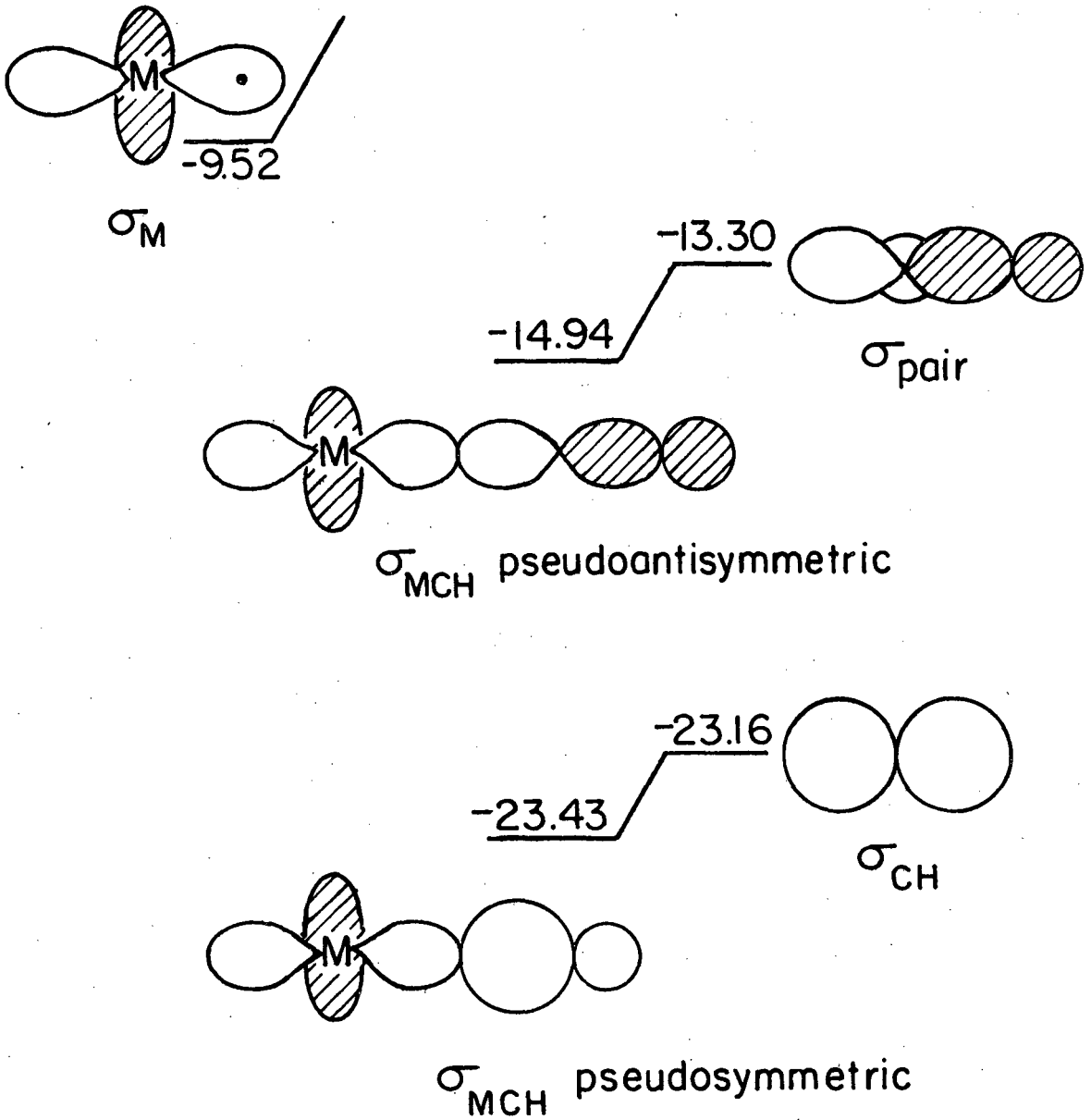

XBL 822-5233

Fig. 3

This report was done with support from the Department of Energy. Any conclusions or opinions expressed in this report represent solely those of the author(s) and not necessarily those of The Regents of the University of California, the Lawrence Berkeley Laboratory or the Department of Energy.

Reference to a company or product name does not imply approval or recommendation of the product by the University of California or the U.S. Department of Energy to the exclusion of others that may be suitable.

TECHNICAL INFORMATION DEPARTMENT
LAWRENCE BERKELEY LABORATORY
UNIVERSITY OF CALIFORNIA
BERKELEY, CALIFORNIA 94720